JOURNAL OF SPACECRAFT AND ROCKETS
Vol. 34, No. 2, March–April 1997

Contamination Experiments in the Midcourse Space Experiment

O. Manuel Uy,* R. C. Benson,† R. E. Erlandson,‡ M. T. Boies,§ and J. F. Lesho¶
Johns Hopkins University, Applied Physics Laboratory, Laurel, Maryland 20723-6099
G. E. Galica** and B. D. Green††
Physical Sciences, Inc., Andover, Massachusetts 01810
B. E. Wood‡‡
Arnold Engineering Development Center, Arnold Air Force Base, Tennessee 37389-6400
and
D. F. Hall§§
The Aerospace Corporation, El Segundo, California 90009-2957

The midcourse space experiment satellite is a space-based sensor platform designed to collect earth and atmospheric remote sensing and astronomy data in support of ballistic missile defense and civilian science objectives. Because of the potential adverse effects of contamination on the main optical sensors, the satellite contains a suite of contamination-monitoring instruments designed to completely characterize the source, generation, and mechanisms of contamination of space optics and to validate preflight contamination models. Descriptions of these contamination instruments, their calibration and testing, and the ground test data collected are presented. The sensitivity to contamination of the main optical sensors, which are imagers and interferometers in the infrared, visible, and ultraviolet spectral regions, are also discussed.

Nomenclature

I_c = collected current, A
I_0 = incoming current, A
m/z = mass-to-charge ratio
V_a = initial drift space potential, V
V_{a+b} = second drift space potential, V
V_E = ion energy, V
V_R = retarding potential, V
V_s = stopping potential, V
V_{sc} = cutoff potential (voltage at which ion current goes to zero), V

Introduction

THE midcourse space experiment (MSX) satellite, with an expected lifetime of 5 years, was launched on a Delta II rocket on April 24, 1996, from the Western Test Range at Vandenberg Air Force Base into a sun-synchronous orbit at an altitude of 903 km and an inclination of 99.36 deg. It is primarily a long-term space-based data collection experiment on the phenomenology of target detection and tracking. In addition, it will perform various experiments in support of science objectives on astronomy as well as Earth and atmospheric sensing.[1] Onboard instrumentation includes the space infrared imaging telescope (SPIRIT III) provided by the Space Dynamics Laboratory of Utah State University, the ultraviolet and visible imagers and spectrographic imagers (UVISI) and the contamination experiments provided by The Johns Hopkins University, Applied Physics Laboratory (JHU/APL), the space-based visible (SBV) telescope provided by Massachusetts Institute of Technology's Lincoln Laboratory, and the onboard signal and data processor experiment provided by Hughes Aircraft Company. A more complete description of the spacecraft, its associated hardware, and its scientific objectives has been published previously.[1]

Optical sensor performance is degraded when molecular film and particulates are deposited on mirrors and windows. The major source of this contamination is the spacecraft itself, although condensation of ambient gaseous species is possible at the SPIRIT III operating temperature of 15 K. Self-contamination results from spacecraft materials outgassing in vacuum and from particles either carried into orbit from the ground or generated by materials moving against each other in space. To minimize self-contamination, only low outgassing materials were used in the fabrication of the spacecraft, and a rigorous contamination control plan was implemented during fabrication, testing, and launch procedures. The contamination experiments will monitor the spacecraft environment in orbit to identify contamination sources, assess the effectiveness of the MSX contamination control plan,[2] and validate the preorbit contamination models used to predict the contamination environment.[3]

Instrumentation

The effectiveness of the MSX contamination control plan,[2] which has been implemented throughout design, materials selection, fabrication, and handling, will be evaluated in actual orbital contamination "performance" with a suite of contamination monitoring instruments. The seven space-qualified instruments are total pressure sensor (TPS), neutral mass spectrometer (NMS), ion mass spectrometer (IMS), cryogenic quartz crystal microbalance (CQCM), temperature-controlled quartz crystal microbalances (TQCMs), xenon flashlamp experiment (XFE), and krypton flashlamp experiment (KFE).

Presented as Paper 96-0219 at the AIAA 34th Aerospace Sciences Meeting, Reno, NV, Jan. 15–18, 1996; received April 15, 1996; revision received Dec. 2, 1996; accepted for publication Dec. 7, 1996.

*Principal Staff Chemist, Technical Services Department, 11100 Johns Hopkins Road. Member AIAA.
†Principal Staff Chemist, Applied Research and Technology Department, 11100 Johns Hopkins Road. Member AIAA.
‡Senior Staff Physicist, Space Department, 11100 Johns Hopkins Road. Member AIAA.
§Senior Staff Engineer, Space Department, 11100 Johns Hopkins Road. Member AIAA.
¶Senior Staff Engineer, Technical Services Department, 11100 Johns Hopkins Road.
**Senior Scientist, Applied Sciences Division, 20 New England Business Center. Member AIAA.
††Vice President, Applied Sciences Division, 20 New England Business Center. Senior Member AIAA.
‡‡Senior Engineer, Arnold Engineering Development Corporation Operations Group, Sverdrup Technology, Inc. Associate Fellow AIAA.
§§Senior Scientist, Materials Group, P.O. Box 92957. Member AIAA.

Total Pressure Sensor

The design of the TPS (Fig. 1) is based on the inverted Redhead gauge or cold-cathode gauge,[4] which had previously flown in numerous spacecraft such as the plasma diagnostic experiment.[5–7] This gauge, however, has been modified for measuring pressures as low as 1×10^{-10} torr to measure the expected ambient pressures between 10^{-6} and 10^{-11} torr. The cold-cathode gauge has been the preferred pressure sensor for most spaceflight missions because of its inherently rugged construction and the absence of a hot filament for generating electrons. Such filaments are often the life-limiting component for pressure sensors (and mass spectrometers) on long-duration spacecraft such as MSX. Coupled with the higher sensitivity to low pressures, however, is the difficulty of starting the ionization process at the lower gas densities; thus, the TPS will not be turned off in orbit unless an emergency or some unforeseen event such as a power failure occurs. The TPS can be turned on again at pressures as low as 1×10^{-10} torr but with a delay of a several seconds.

The instrument was calibrated at the National Institute of Standards and Technology (NIST) for the gases H_2, He, H_2O, N_2, O_2, and Ar for pressures ranging from 1×10^{-4} to 1×10^{-10} torr. It was also cross calibrated (Fig. 2) with the NMS total ion current monitor so that pressures lower than 1×10^{-10} torr can be obtained with the NMS toward the latter half of the MSX mission, when the TPS may not have the necessary sensitivity.[8–10]

NMS

The NMS (Fig. 3) had flown in space previously as part of the space transportation system (STS) induced environment contamination monitor. A detailed description of the instrument has been published.[11] Similar mass spectrometers were also flown on the Atmospheric Explorer C, D, and E[12] and on the Dynamics Explorer Satellites.[13]

The NMS is a closed-source quadrupole instrument with an electron-bombardmention source. Chemical species enter the mass spectrometer antechamber through a knife-edged orifice. In the antechamber, the species come into thermal equilibrium through multiple collisions with the walls before being ionized by conventional electron-impact techniques. The ionized species are then collimated into the quadrupole analyzer, which uses both a dc and rf voltage

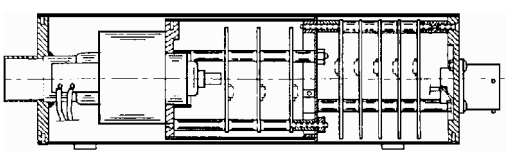

Fig. 1 MSX TPS.

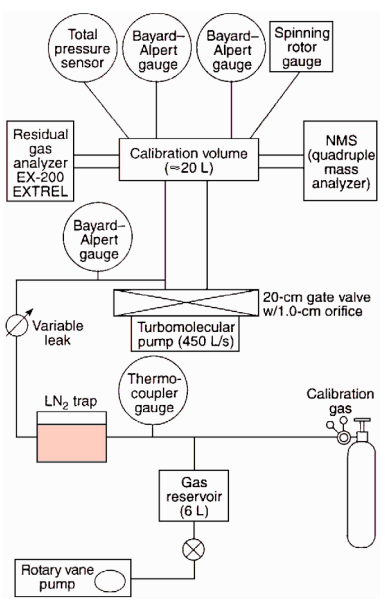

Fig. 2 Schematic of the cross-calibration chamber used for the TPS and NMS.

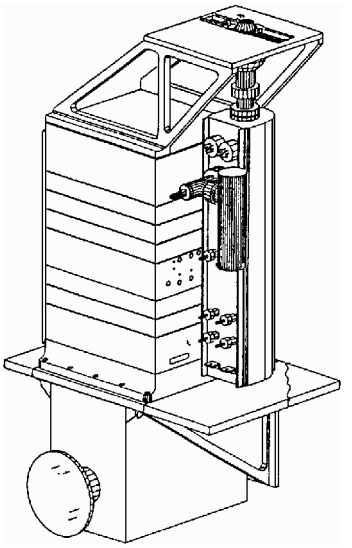

Fig. 3 MSX NMS.

across four rods to select a specific m/z. The instrument can operate over the range 1–150 m/z. Ions with the selected m/z then pass through the quadrupole analyzer and are detected with an electron multiplier. The spectrometer can be operated in either a scanning mode with 1- or 1/16-m/z steps or a single-ion monitoring mode in which selected peaks are monitored continuously for increased sensitivity.

Calibration was performed in an all-metal turbopumped vacuum chamber (Fig. 2).[14] The typical base pressure of this system was approximately 5×10^{-9} torr. A quadrupole partial pressure analyzer and two Bayard–Alpert ionization gauges, previously calibrated in the NIST calibration chamber, were used to provide transfer standards. The ion gauges were operated with a 0.875-mA emission current. Calibration gases were introduced into the chamber through a precision leak valve, which was connected to a ballast tank. The partial pressure of the calibration gas in the vacuum chamber was controlled by varying the ballast tank pressure. By this technique, the calibration gas partial pressure was varied from the base pressure up to 1×10^{-6} torr (limited to 1×10^{-7} torr in the case of reactive gases) by factors of three at each step.

To provide a reproducible baseline, the NMS was repeatedly calibrated in helium. Helium, the predominant naturally occurring species on orbit, is not reactive and therefore does not produce chemical changes in the filament or the source region. The NMS sensitivity is reproducible within 20%, even after the NMS has been exposed to a highly reactive gas such as oxygen or water vapor. The two filaments have slightly different sensitivities.

The characterization of the NMS in water vapor is extremely important to the MSX program because it is expected to be the primary contaminant in the spacecraft environment. The spacecraft itself will be the primary source of the water vapor, which previously had adsorbed onto the blankets and exposed surfaces of all elements of the spacecraft.

The deposition of water vapor on the sensitive cryogenic optical surfaces and the subsequent loss of sensor performance are of paramount concern. Calibration of the NMS in water vapor was accomplished by means of a NIST prototype water vapor source connected to the vacuum chamber through a precision leak valve. The instrument response was limited to a maximum pressure of 10^{-7} torr to protect against failure of the NMS filament. The NMS response was strongly time dependent, with equilibration times ranging from 1 to 2 h. In addition, other gas species were generated within the vacuum chamber and detected by the NMS, especially hydrogen, carbon monoxide, and carbon dioxide. The response of the Bayard–Alpert gauges to these gases was determined before calibration of the NMS. Consequently, it was possible to correct the gauge reading for the presence of these species to determine the gauge response to water vapor alone.

The response of the NMS to water is basically linear, although large amounts of other gases were generated. Note that the operation

of a single gauge can lower the expected water vapor partial pressure by several percentages because of water vapor reactivity with the filaments. During NMS calibration, two ionization gauges and two partial pressure analyzers, including the NMS, were operated continuously. Thus, ample opportunity existed for water vapor to interact with the filaments to produce large amounts of H_2, CO, CO_2, and other gases. Initially, these other gases increased at a rate similar to water vapor but were evidently limited by a process that was reaching saturation in the chamber. Some contribution because of increased desorption of these contaminant gases from the walls was also present, because these gases increased somewhat during calibration of helium, argon, and other nonreactive gases. The sensitivity of the NMS (10-mA filament emission current, filament 1) to water vapor was 4×10^{10} counts/torr but was slightly pressure dependent. Thus, the NMS water vapor sensitivity is comparable to the sensitivities for well-behaved nonreactive gases such as nitrogen and argon, for each of which the NMS had a sensitivity of $1\text{–}4 \times 10^{11}$ counts/torr, depending on filament emission and NMS detector configuration.

The NMS was also calibrated with other molecular species that will be present on orbit. Argon and hydrogen will be the predominant contaminants in the spacecraft environment because they are the byproducts of the SPIRIT III sensor cooling system. Although atomic oxygen will be present on orbit, it will react on surfaces and remain adsorbed or recombine to form molecular oxygen; hence, O_2, was a calibration gas. Finally, nitrogen was used in instrument testing as the standard by which other mass spectrometers could be compared to the NMS.

The NMS analyzer tube has been backfilled with trace amounts of four noble gases: helium, argon, krypton, and xenon. These gases provide the means of comparing ground and orbital performance. Their concentrations are well known and were measured monthly during the integration and testing phase of spacecraft development. Before the NMS aperture cover is opened, the instrument will be operated to determine its on-orbit performance.

IMS

The IMS (Fig. 4) is a Bennett 5-3 cycle rf mass spectrometer designed to record the ion flux as a function of mass.[15] It is similar in design to the instruments flown on the Atmospheric Explorer C satellite,[16] the STS-51F,[17] and the Pioneer-Venus Orbiter.[18] The Bennett IMS consists of a spectrometer tube and associated electronics. The spectrometer tube consists of a lightweight anodized A sensor housing with polyimide spacers and fine-mesh grids attached to stainless steel grid rings to which various rf and dc voltages are applied. The spacing between the grids in the analyzer sections and rf applied to the grids determine the ion mass selected by the spectrometer. A more complete description of the IMS and the calibration techniques can be found elsewhere.[19]

The experimental setup of the IMS calibration is shown in Fig. 5. An ion gun and the IMS sensor tube are mounted on opposite ports, with their orifices along the center line of the cylinder. The IMS electronics were located outside the vacuum chamber. A coaxial transparent retarding potential analyzer (RPA) is mounted on the inside flange in front of the IMS sensor orifice to measure the total ion flux entering the sensor. An ion flux of different ion constituents is produced by leaking various calibration gases into an ion gun. A schematic of the ion source and the RPA calibration equipment is shown in Fig. 6.

The objective of the IMS calibration[19] is to determine instrument efficiency as a function of V_s. The efficiency is the ratio of I_c to I_o as recorded by the RPA. Ion efficiency varies from one ion species to another, which results in the requirement to calibrate the IMS for all ion species of interest. During each spectral calibration, V_s will be varied over a range from 45 V to V_{sc}. IMS calibration was performed with seven different gases (H_2, He, H_2O, N_2, O_2, Ar, and CO_2), which were ionized in an ion gun. Reactions in the ion gun also produce other ion constituents related to the primary gas. The IMS ion current will be recorded as a function of V_s for each ion species (fundamental) and harmonically identified by the IMS peak picker electronics.

The expected ionospheric and contaminant species were used to identify the types of ions to be used in the IMS spectral calibration. The ionospheric species at the MSX altitude of 900 km are predominantly H^+, He^+, and O^+ based on the international reference ionosphere. The contaminant ion species and flux expected in the vicinity of long-duration satellites such as MSX are not presently

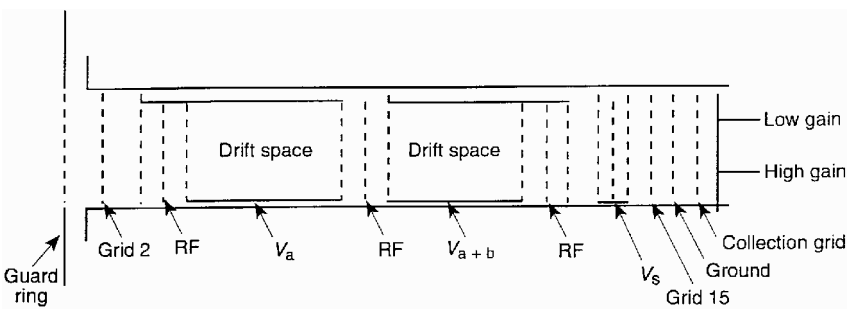

Fig. 4 Schematic of the Bennett 5-3 cycle IMS tube.

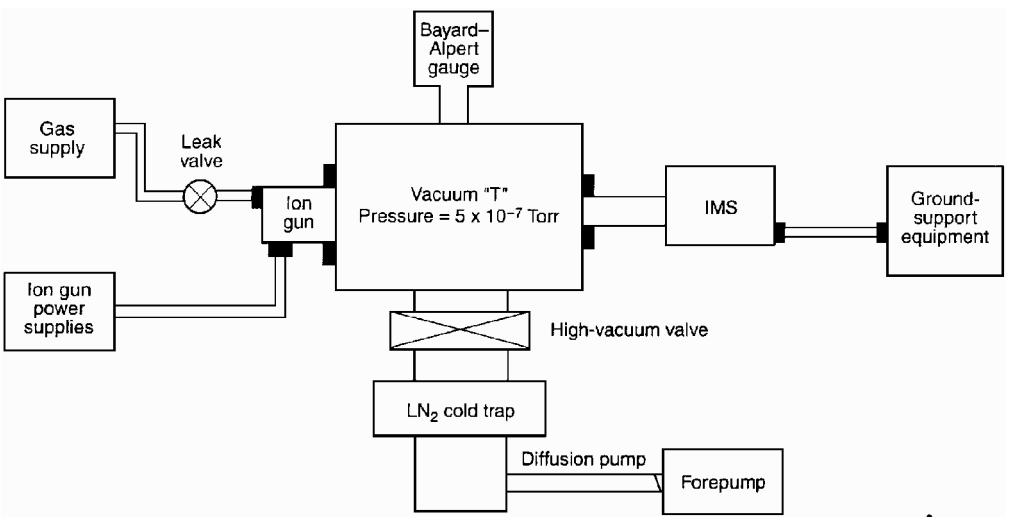

Fig. 5 Schematic of the IMS calibration facility.

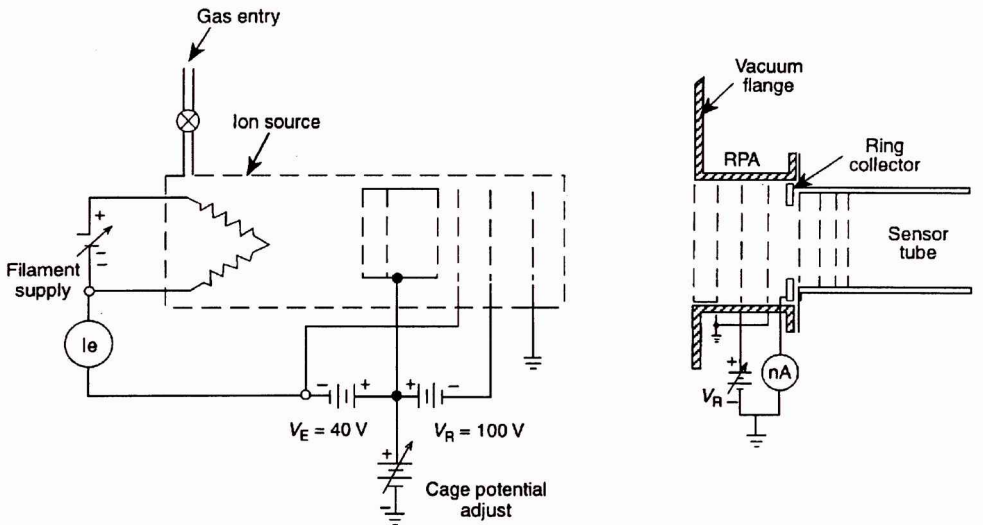

Fig. 6 Ion source and RPA used in the IMS spectral calibration.

known. Previous observations of contaminant ions were obtained from the Space Shuttle. The dominant species observed near the Space Shuttle include H_2O^+, H_3O^+, OH^+, and CO_2^+ (Refs. 17, 20, and 21). The induced environment of the Space Shuttle, however, differs significantly from the induced environment of unmanned satellites. Those expected ion species near the MSX spacecraft are based on theoretical considerations, because relevant observations do not exist. The theoretical considerations include the dominant neutral contamination species and charge exchange cross sections. The dominant neutral outgassing species are expected to be H_2O during the early phase of the mission and H_2 from the cryogen vent. Charge exchange reactions with ionospheric O^+ are expected to lead to H_2O^+ and H_3O^+ contaminant ions.

CQCM

The Mark 16 model CQCM (Fig. 7) is a mass sensor and can detect condensed masses on the order of 10^{-9} g/cm^2. It was designed to operate at temperatures as low as 4 K. The CQCM uses two quartz crystals (to minimize temperature effects) that are made to oscillate at 10 MHz and are positioned so that one crystal is exposed to the external environment, whereas the reference crystal is protected from any deposition. The difference in frequency is directly proportional to the mass condensed on the exterior crystal. The quartz crystals were previously exposed to 100 kGy (Si) in a cobalt-60 source at JHU/APL to minimize radiation-induced frequency degradation during the time in orbit. The MSX CQCM is located adjacent to and thermally coupled with the cryogenically cooled primary mirror of the SPIRIT III telescope. It will be used to monitor the deposition of contaminants on the interior optics and, with associated bidirectional reflectance distribution function data, will be used to predict the degradation in performance of the mirror. The CQCMs were calibrated/characterized at temperatures as low as 10 K in a cryogenic calibration facility at the Arnold Engineering Development Center, Tullahoma, Tennessee. The results of these calibrations and the correlations of the QCM measurements with optical effects have been reported.[22–24] Since installation in the SPIRIT III telescope, the CQCM has been a valuable tool in monitoring the mirror status in cryogenic testing of SPIRIT III at USU, thermovacuum testing at the Goddard Space Flight Center, and preflight measurements at Vandenberg Air Force Base.

TQCM

The TQCMs (Fig. 8) were designed to operate routinely at temperatures as low as 203 K and as high as 343 K. The temperatures are controlled by a Peltier cooler/heater unit, which is built into the Mark 10 TQCM sensor head. As with the CQCM, one of the two crystals is exposed to the environment; the other is the reference crystal and is protected. The crystals operate at a frequency of 15 MHz, which makes the TQCM approximately 2.25 times more sensitive than the CQCM. Six TQCMs were calibrated/characterized

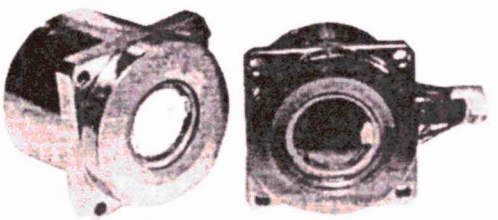

Fig. 7 MSX CQCM.

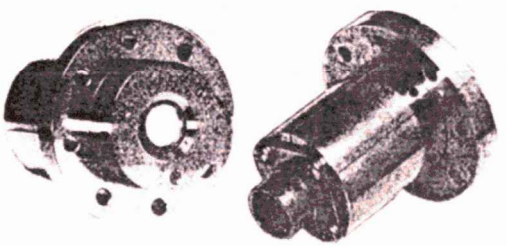

Fig. 8 Mark 10 model TQCM.

at the Arnold Engineering Development Center with the same cryogenic test facility as discussed for the CQCM, which provided the necessary vacuum and low temperatures. The calibration information has been previously reported.[25–27]

There are four TQCMs mounted on the exterior of MSX with locations of $(+y, +z)$, $(+z)$, $(+y, -z)$, and $(+x, +z)$. The coordinates are based on the $+x$ being the axis toward which the optical telescopes are pointing. During quiescent or "parked" attitude, the $+z$ is the velocity "ram" direction. Three TQCMs are mounted with thermal radiators at the approximately orthogonal axes of the MSX spacecraft with a 128-deg field of view of space. The other TQCM is located slightly below the first three on the instrument section and is facing directly down with the electronic section and most of the solar array in its field of view. All TQCMs will be maintained at a temperature of approximately $-50°$ C (223 K) throughout the mission. This temperature was calculated to be cooler than any external source such as the multilayer insulation, electronic boxes, and other noncryogenically cooled surfaces of the spacecraft and is cold enough to condense most hydrocarbons emanating from MSX. Outgassing predictions have been reported.[3]

XFE

The XFE characterizes the MSX near-field particulate contamination environment. The experiment can detect particles smaller than 1 μm and can determine cross-field particle velocities from 0.1 to 50 m/s. The measurement is based on Mie scattering of visible

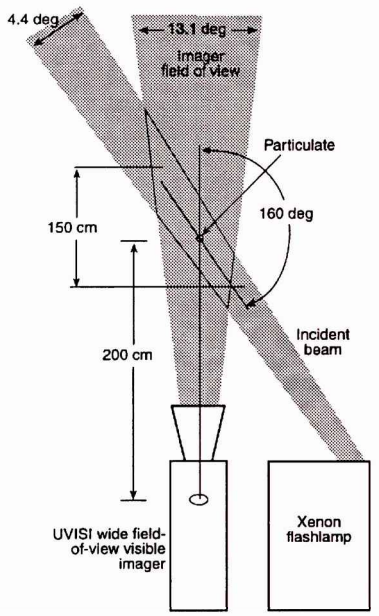

Fig. 9 Schematic of the XFE with the UVISI.

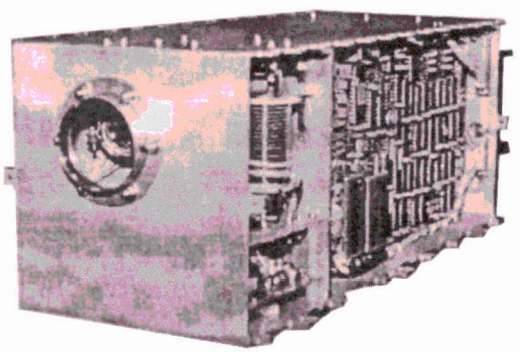

Fig. 10 MSX XFE.

radiation. The near field is illuminated with visible radiation from the xenon flashlamp; the resulting scattered radiation is observed with the UVISI wide field-of-view visible imager (UVISI IVW; Fig. 9). The intensity yields information about the size and number of particles. The tracks of scattered radiation imaged by the UVISI IVW provide information about the velocity and trajectory of those particles.

The xenon flashlamp (Fig. 10) measures $18 \times 15 \times 41$ cm and has a mass of 7.2 kg. It incorporates a xenon illuminator with an integral reflector, associated control electronics, and an optical flux monitor. The illuminator itself has an integral prefocused reflector, which provides a beam divergence of 4.4 ± 0.4 full-width, half-maximum and 11.8 ± 0.8 deg full-width, tenth-maximum. The peak intensity of this flashlamp is 1×10^{20} photons/s over the visible wavelength region (400–900 nm). The intensity of each flash is measured by an onboard optical monitor, with an uncertainty of $\pm 11\%$. The flashlamp is operated in a burst mode, where each 0.5-s burst consists of nine 11-ms flashes of the lamp. The bursts repeat at a 1-Hz rate. This flash pattern provides a modulation in the particle signature within a single image, thereby allowing the angular velocity of the particles to be determined.

The UVISI IVW has a field of view of 10.5×13.1 deg, a pixel size of 750×890 mrad, a 244×256 image output (when operated at a 2-Hz frame rate), and a collecting area of 25 cm^2. One IVW filter wheel position contains a lens that refocuses the imager at the region of intersection of the xenon flashlamp beam and the IVW field of view (2 m from the IVW first optic). The xenon flashlamp and the UVISI IVW are calibrated independently. The primary standard used for the flashlamp calibration is a 1000-W tungsten irradiance standard with a NIST-traceable calibration against which the spectral irradiance of the xenon flashlamp is compared. In addition, properties including pulse-to-pulse intensity variation, temporal pulse shape variation, and temperature and voltage effects are characterized.

After completion of the individual instrument calibrations, an end-to-end performance test was carried out with the two instruments in joint operation. The test was performed in a clean room that is certified to class 10,000 but that typically approaches class 1000. The xenon flashlamp and the UVISI IVW were bolted to a mock spacecraft instrument pallet, which ensured that the instruments would be in their relative flight geometry (see Fig. 9).

To control contamination of the UVISI, the IVW aperture cover remained in place during testing. The cover is equipped with a window through which the sensor views the illuminated volume with a reduced field of view (5.5 deg circular). Particle measurements made during the early phase of the mission will also be performed with the IVW observing through its aperture cover window. The background for the IVW field of view was provided by a set of black plates. Although the baffling and light-blocking measures were quite effective, some reflected stray light was present in the images. In addition, Mie scattering from very small particles and Rayleigh scattering limited the ultimate sensitivity of the laboratory measurements.

Three sizes of latex spheres (50-, 14-, and 5-μm radius) were introduced into the measurement volume. The spheres are provided as a suspension in a solvent. The 5-μm spheres were introduced with a nebulizer that evaporates the solvent and essentially dispenses particles on a current of air. The larger spheres were introduced with a pipette after evaporation of the solvent in ambient air.

Figures 11a and 11b show an image and the corresponding surface plot of a 14-μm particle traversing the field of view. The single particle was repeatedly illuminated as it moved from the center toward the upper-left-hand corner of Fig. 11a. The light pulses are 11 ms in duration and occur 55 ms apart. By measuring the pixel separation of the particle signatures, one can determine the cross-image component of the velocity, in this case about 10 cm/s. Figure 11b shows a three-dimensional plot of Fig. 11a, which illustrates the signal-to-noise ratios involved in this measurement.

The variation in the intensities of the individual signatures is the result of the experiment configuration. During laboratory measurements, the UVISI IVW made observations through its aperture cover window; therefore, the field of view is vignetted to an unquantified degree and reduced to 5.5 deg. As a particle approaches the edge of the vignetted field of view, the effective sensitivity to that particle is reduced. During ground testing, the dominant background originated from stray xenon flashlamp radiation reflected from the backdrop in the IVW field of view. During flight, this stray light background will not come into play, and the dominant background will be the celestial radiance from the background stars.

Figure 12 shows simulated scenes that demonstrate how the flight data will appear. The panel on the left shows a simulated star scene for the UVISI IVW in its standard configuration, i.e., the star intensities follow the correct magnitude distribution for a particular galactic latitude (30 deg in this case), but the scene itself does not correspond to actual stars.[28] The middle panel shows the same scene as it would appear with the near-field focus lens in place and with a 1.5-μm particle moving through the field of view (including Poisson noise). With the near-field focusing lens in place, point sources at

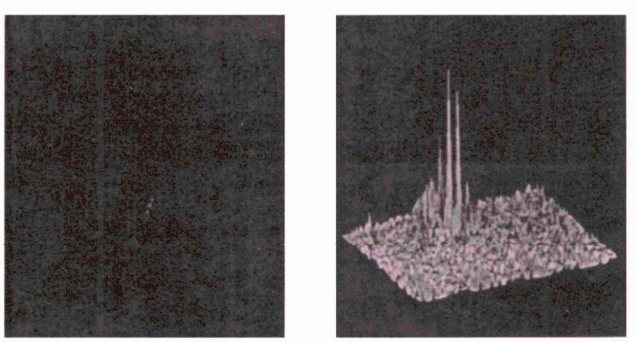

a) 14-μm particle image **b) Surface plot**

Fig. 11 XFE.

Fig. 12 XFE: simulated star scene (left), blurred stars with particles (middle), and background-subtracted scene (right).

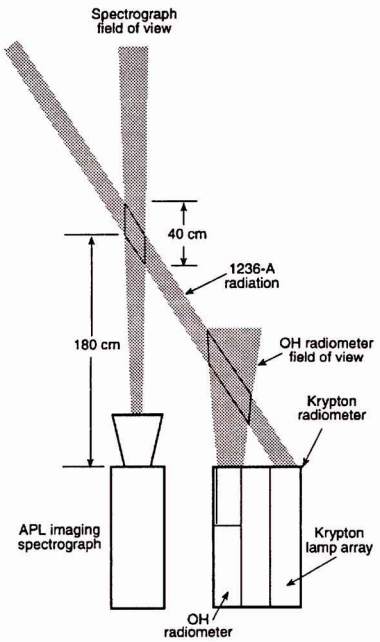

Fig. 13 Schematic of the XFE with the visible imager.

infinity form a blurred circle of approximately 26 pixels in diameter (90% encircled energy) on the focal plane. Point sources in the near field are nearly in focus, forming blurred circles ranging from 3 to 6 pixels in diameter over most of the illuminated volume. The right-hand panel of Fig. 12 shows the previous image after subtracting an identically simulated background image (equivalent to postacquisition frame-to-frame subtraction), thereby leaving only the particle signature and the Poisson noise in the celestial background. The particle signature is clearly visible in the background-subtracted image.

KFE

The KFE yields a spectroscopic measurement of the local H_2O density. The technique involves photodissociation of water vapor in the near field of the spacecraft with visible ultraviolet (VUV) radiation and measurement of the subsequent emission from the electronically excited products. The intensity of the resulting radiation is directly proportional to the density of water vapor. The experiment is shown schematically in Fig. 13. The krypton lamp and radiometer units include a VUV source that dissociates the H_2O molecules. Chemiluminescence is detected simultaneously by a filtered photometer (the radiometer part of the lamps and radiometer) and by one of the MSX UVISI spectrographic imagers (UVISI SPIM3). The SPIM3 spectral measurement (2-nm resolution) provides a positive identification that the radiating species is OH.

When a water molecule absorbs a photon in the 105- to 135-nm wavelength region, it dissociates with unit quantum yield into a hydrogen atom and either a ground state or an electronically excited state OH radical.[29] The excited state OH ($^2\Sigma^+$) radical then fluoresces promptly in a rovibronic band at 306.5 nm.[30] This chemistry forms the basis for the operation of the krypton lamp and radiometer unit.

The krypton lamp and radiometer section shown in Fig. 14 consists of a baffle, a 305- to 325-nm interference filter, a focusing lens, a field stop that defines the field of view, a test source, and an integrated photodetector (photomultiplier, high-voltage power

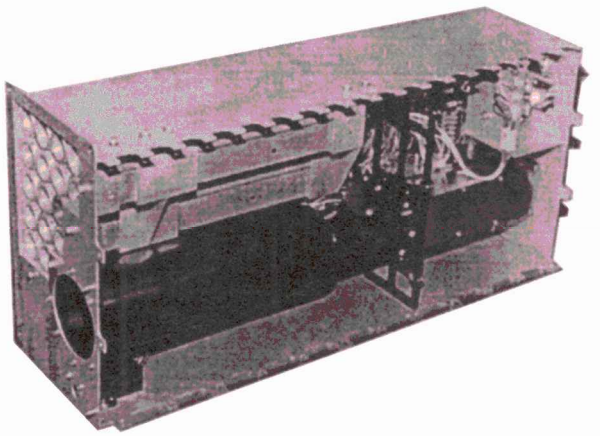

Fig. 14 MSX KFE.

supply, and pulse-height discriminator). The krypton lamp section consists of 16 individual krypton line source lamp modules (123.6 nm), each independently focused and aligned via MgF_2 lenses. The lamps are of an rf-excited (100 MHz) electrodeless discharge design. Each lamp module contains its own control circuitry and flux monitor. The lamps flash at a repetition rate of 1 Hz with a pulse width of 500 ms (synchronized to major and minor frame marks). The remainder of the instrument houses a sun sensor (to protect the radiometer) and control electronics. The main electrical component is the housekeeping board, which performs command and telemetry functions and also supplies regulated power to the radiometer and lamp modules. The instrument dimensions are 15 × 22 × 48 cm, and its mass is 7.8 kg.

The krypton lamps and the OH radiometer section are fully calibrated and characterized independently. In addition, the instrument is calibrated as a unit. Because the UVISI SPIM3 plays a semiquantitative role in this measurement, by simply providing a spectral identification of the radiating species, no joint ground testing was performed.

The absolute VUV irradiance of the krypton lamps was measured with a CsI photodiode having a NIST-traceable calibration. In addition, the lamps were fully characterized, including measurements of spectral properties, focus and alignment, beam divergence, temperature effects, and voltage effects. The OH radiometer was calibrated for absolute radiance sensitivity with a 1000-W tungsten irradiance standard having a NIST-traceable calibration. It was also fully characterized for linearity of response, dark current, field of view, temperature effects, and voltage effects.

The krypton lamp and radiometer unit was calibrated for H_2O responsivity in a thermal-vacuum facility chamber. This facility is an ultraclean, all stainless steel, all metal-sealed chamber. Rough vacuum is achieved with a dry-sealed, multistage, mechanical piston pump. High vacuum is achieved with a 3000 L/s cryopump. The chamber is equipped with a Bayard–Alpert gauge, calibrated by NIST for responsivity to water vapor and N_2 with an accuracy of better than ±10% for each species. In addition, the chamber is equipped with a residual gas analyzer (RGA). After initial pumpdown the chamber background pressure is dominated by the partial pressure of H_2O ($\geq$ 90% mole fraction). The RGA provides a quantitative measure of the H_2O mole fraction, which, with the total pressure determined by the Bayard–Alpert gauge, yields the H_2O partial pressure.

The instrument was placed in the chamber with appropriate baffling to reduce scattered light. The chamber was evacuated, and measurements were taken as the pressure slowly decreased. The dynamic range of the krypton lamps and radiometer spans approximately six decades. However, the H_2O calibration could be performed over only approximately two decades in the center of the dynamic range (10^9–10^{11} H_2O molecules per cm^3). The calibration is extrapolated over the entire dynamic range based on the independent calibrations and characterizations of the krypton lamps and the OH radiometer. From this calibration, the instrument constant is determined with an uncertainty of ±23%.

Table 1 MSX primary optical instrument specifications

Sensor	Function	Spectral region, μm	Resolution	Field of view, deg
UVISI imagers	Staring/scanning			
Ultraviolet wide		0.11–0.18	820 μrad	1.28 × 1.59
Ultraviolet narrow		0.18–0.30	90 μrad	10.5 × 13.1
Visible wide		0.38–0.30	820 μrad	1.28 × 1.59
Visible narrow		0.30–0.90	90 μrad	10.5 × 13.1
Spectrographic imagers	Spatial/spectral	0.113–0.902	0.5–4.3 nm	1.0 × 1.0
SBV	Staring	0.30–0.90	60 μrad	1.4 × 6.6
SPIRIT III radiometers	Scanning	6.0–10.9		
		4.22–4.36		1 × 0.75
		4.34–4.45	90 μrad	1 × 1.5
		11.1–13.2		1 × 3
		13.5–16.0		
		18.1–26.0		
Interferometer	Spectral (six filters)	2.5–28	2, 3.9, 20 cm^{-1}	0.86

Given the calibrated instrument constant and the calibrated responsivity of the OH radiometer, one can calculate the performance of the instrument when viewing the celestial background. In flight, the dominant background will be celestial radiance from the background stars. A minimum detectable H_2O density of 1.6×10^7 molecules per cm^3 with a signal-to-noise ratio of 3 is predicted.

Main Optical Sensors

In addition to the dedicated contamination instruments already described, the primary optical sensors on MSX will be able to measure the contamination environment by observing changes in the radiant signature levels as particles and molecules pass through their fields of view. Contamination transported onto the optical surfaces of the primary sensors will also be detected by sensor optical performance degradation. The performance specifications of the MSX primary optical instruments have been reviewed elsewhere[1,31,32] and are summarized in Table 1.

The UVISI imagers and interferometers provide the spectral resolution necessary to discriminate molecular contamination features from background emissions. Contamination molecules will be excited into emitting molecular states by solar fluorescence and photolysis (in the ultraviolet and visible) and by collisional and thermal excitation processes (in the infrared). The observed molecular signatures will be compared with synthetic emission predictions to first identify the emitting species and then extract internal (electronic, vibrational, rotational) population distributions. These distributions will provide insight into the excitation mechanisms.

The radiometers/imagers detect light over broad spectral bands and more easily detect less spectrally structured particle emissions. The SBV and the UVISI imagers are staring array systems with selectable integration periods. The SPIRIT III radiometer linear array fields of view can be scanned to create a two-dimensional pseudoimage. The fields of view of these sensors were carefully coaligned before launch to permit accurate observation and comparison of phenomena in different spectral bandpasses. Particle tracks observed in the imagery will permit particle position, velocity, and trajectory reconstruction. Observation of the same particle in several spectral bandpasses will potentially permit particle composition identification as described below.

Contamination deposition on the primary instrument optical surfaces will also be assessed. The SBV has incorporated an in situ scatter source to permit monitoring of mirror quality degradation in a relative sense over the duration of the mission. The CQCM sensor has proven invaluable in assessing the level of accretion on the cryogenic primary mirror of SPIRIT III. Careful experiments are planned on orbit to use the angular dependence of the off-axis rejection of the radiance from the Earth limb and moon to monitor performance degradation of all these telescoped optical systems throughout the lifetime of the mission.

The optical properties for materials likely to be produced by orbital erosion, abrasion, thermal cycling, and outgassing have been assembled. These materials include silver, aluminum, alumina, carbon, carbon dioxide and water ices, silicon dioxide, and titanium dioxide. Metal films of silver and aluminum are likely to be created from the degradation of coatings on reflectors and insulation. Alumina is formed by solid-rocket motor exhaust and by the orbital oxidation of aluminum. Amorphous carbon soot is representative of high-emissivity black optical coatings that have been released by abrasion. Silicon dioxide is a likely contaminant during ground processing that is brought to orbit. Titanium dioxide is a common pigment in white paints that is released as its binder is degraded. The wavelength-dependent scattering indices of these species produce spectrally structured radiances. Details of this calculation have been described elsewhere.[33] Each of the eight species considered possesses a unique identifiable radiant intensity spectrum. Thus, particles of these compositions could be identified from the simultaneous observations of the MSX primary sensors.

Particles will leave spacecraft surfaces with a wide range of velocities. Whereas thermal desorption and mechanical abrasion will favor slowly moving particles,[34,35] micrometeorite impact can produce rapidly moving particles.[36] Particles leaving spacecraft surfaces will be accelerated by atmospheric drag (and magnetic forces if charged). They are expected to leave the surface with a velocity relative to the spacecraft. Molecules of the tenuous upper atmosphere collide with the particles at an 8-km/s velocity and exert drag, forcing them to slow relative to the atmosphere (but accelerate away from the spacecraft). Particle acceleration in the spacecraft frame depends on atmospheric density and composition (these quantities will be measured by the NMS and TPS aboard MSX). Particles will be in the optical field of view either by having a trajectory passing directly through the near-field observed volume or a trajectory initially to the windward of the optical axis that is swept back into the observation volume. Particles are expected to remain in the vicinity of the spacecraft and be accelerated over a 100- to 10,000-s period. Thus, particles could be resident in the field of view for an entire data collection event.

Automated algorithms were developed to extract position and velocity of particles observed in the MSX imagery database. Automated analysis will be essential to permit even cursory examination of the large MSX database for contamination feature identification.[33]

Summary

The suite of instruments composing the MSX contamination experiment has been well designed for study of the phenomenology of gaseous and particulate generation in orbit. Each of the contamination instruments has been calibrated on the ground so that the flight data can be reported in quantitative engineering units. Of interest are the level of molecular and particulate environment during early missions (first 2 weeks after launch), their decay rates over the mission life of 5 years, and their effect on the performance of the optical sensors as well as the electrical output of the solar arrays. It is also anticipated that discrete contamination events will be measured, such as particulate size distribution, counts and decay rate during each of the optical instruments' door openings, and release of several calibration spheres. On the basis of knowledge of the materials present, the actual contamination measured, and the contamination levels predicted by our models, it is anticipated that we will modify the models to fit the data and thus come up with a validated contamination model for this type of spacecraft. In addition, the neutral

and ion mass spectrometers, which will be continuously taking mass spectral data from day 2 through mission year 5 should provide a large database of the Earth's ambient atmosphere at the MSX altitude of 900 km for the Mass Spectrometer Incoherent Scatter and International Reference Ionosphere atmospheric models currently in use by the space science community.

Acknowledgments

The MSX spacecraft was built, integrated, and tested by the Johns Hopkins University, Applied Physics Laboratory for the Ballistic Missile Defense Organization with Bruce Guilmain as MSX Program Manager, A. T. Stair Jr. of Visidyne Corporation as Chief Scientist, J. D. Mill as MSX Technical Operations Manager, and Max Peterson as Spacecraft Program Manager. We would also like to acknowledge the instrument vendors, Peter Simeth of Sentran Company in Santa Barbara, California, for the total pressure sensor; George Carignan of the Space Physics Research Laboratory at the University of Michigan, Ann Arbor, for the neutral mass spectrometer; Jack Coulson of IDEAs, Inc., Columbia, Maryland, for the ion mass spectrometer; Don and Scott Wallace of QCM Research, Laguna Beach, California, for the cryogenic quartz crystal microbalances; and Orr Shephard of Visidyne Corporation, Burlington, Massachusetts, for the xenon and krypton flashlamps.

References

[1]Mill, J. D., O'Neil, R. R., Price, S., Romick, G. J., Uy, O. M., Gaposchkin, E. M., Light, G. C., Moore, W. W., Jr., Murdock, T. L., and Stair, A. T., Jr., "Midcourse Space Experiment: Introduction to the Spacecraft, Instruments, and Scientific Objectives," *Journal of Spacecraft and Rockets*, Vol. 31, No. 5, 1994, pp. 900–907.

[2]Cranmer, J. H., Sanders, J. T., Jr., Lesho, J. C., and Uy, O. M., "Contamination Control for the Mid-Course Space Experiment, An Overview," *JHU/APL Technical Digest*, Vol. 17, No. 1, 1995, pp. 88–101.

[3]Silver, D. M., "Midcourse Space Experiment Contamination Modeling," AIAA Paper 96-0223, Jan. 1996.

[4]Redhead, P. A., "The Magnetron Gauge: A Cold-Cathode Vacuum Gauge," *Canadian Journal of Physics*, Vol. 37, Nov. 1959, pp. 1260–1271.

[5]Shawhan, S. D., Murphy, G. B., and Pickett, J. S., "Plasma Diagnostic Package Initial Assessment of the Shuttle Orbiter Plasma Environment," *Journal of Spacecraft and Rockets*, Vol. 21, No. 4, 1984, pp. 387–391.

[6]Shawhan, S. D., and Murphy, G. B., "Plasma Diagnostic Package Assessment of the STS-3 Orbiter Environment and Systems for Science." AIAA Paper 83-0253, Jan. 1983.

[7]Pickett, J. S., Murphy, G. B., and Kurth, W. S., "Gaseous Environment of the Shuttle Early in the Spacelab 2 Mission," *Journal of Spacecraft and Rockets*, Vol. 25, No. 2, 1988, pp. 169–174.

[8]Uy, O. M., Benson, R. C., Boies, M. T., Kinnison, J. D., Morgan, J. S., Tison, S. A., Fillipilli, A. R., and Tilford, C. R., "Ground Calibration of the Mass Spectrometer and Total Pressure Sensor in the Midcourse Space Experiment (MSX)," Technical Paper 94-1473, Society of Automotive Engineers, Warrendale, PA, June 1994.

[9]Uy, O. M., Benson, R. C., Boies, M. T., Kinnison, J. D., and Morgan, J. S., "Use of the NIST-Developed Water Calibrator for the Midcourse Space Experiment (MSX) Mass Spectrometer," *Proceedings of the SPIE—The International Society for Optical Engineering*, Vol. 2214, 1994, pp. 316–324.

[10]Burdick, S., Uy, O. M., Erlandson, R. E., Boies, M. T., Lesho, J. F., and Cooper, S. B., "Certification of the MSX Contamination Instrument Data," *Proceedings of the Fifth Annual IR Radiometric Calibration Symposium*, Utah State University Space Dynamic Laboratory, Logan, UT, 1995.

[11]Miller, E. R., and Decher, R., "An Induced Environment Contamination Monitor for the Space Shuttle," NASA TM-78193, Aug. 1978.

[12]Pelz, D. T., Reber, C. A., Hedin, A. E., and Carignan, G. R., "A Neutral Atmosphere Composition Experiment for the Atmospheric Explorer-C, -D, and -E," *Radio Science*, Vol. 8, No. 4, 1973, pp. 277–285.

[13]Carignan, G. R., Block, B. P., Maurer, J. C., Hedin, A. E., Reber, C. A., and Spencer, N. W., "The Neutral Mass Spectrometer on Dynamics Explorer," *Space Science and Instrumentation*, Vol. 5, No. 4, 1982, p. 429.

[14]Boies, M. T., Benson, R. C., Kinnison, J. D., Morgan, J. S., Phillips, T. E., Uy, O. M., and Wilkinson, W., "Cooperative Sensor Calibration: Mid-course Space Experiment (MSX) Neutral Mass Spectrometer and Total Pressure Sensor," *Proceedings of the SPIE International Society of Optical Engineering, Optical System Contamination—Effects, Measurement and Control*, Vol. 2261, 1994, p. 208.

[15]Bennett, W. H., "Radiofrequency Mass Spectrometer," *Journal of Applied Physics*, Vol. 21, Feb. 1950, p. 143.

[16]Brinton, H. C., Scott, L. R., Pharo, M. W., III, and Coulson, J. T., "The Bennett Ion-Mass Spectrometer on Atmospheric Explorer-C and -E," *Radio Science*, Vol. 8, April 1973, p. 323.

[17]Grebowsky, J. M., Taylor, H. A., Jr., Pharo, M. W., III, and Reese, N., "Thermal Ion Perturbations Observed in the Vicinity of the Space Shuttle," *Planetary and Space Science*, Vol. 35, April 1987, pp. 501–513.

[18]Taylor, H. A., Jr., Brinton, H. C., Wagner, T. C. G., Blackwell, B. H., and Cordier, G. R., "Bennett Ion Mass Spectrometer on the Pioneer Venus Bus and Orbiter," *IEEE Transactions on Remote Sensing*, GE-18, Inst. of Electrical and Electronics Engineers, New York, 1980, p. 44.

[19]Erlandson, R. E., Boies, M. T., Uy, O. M., and Grebowsky, J. M., "The MSX Ion Mass Spectrometer: Measurement of Contaminant and Ambient Ions," *Proceedings of the SPIE International Society of Optical Engineering, Optical System Contamination—Effects, Measurement and Control*, Vol. 2261, 1994, pp. 181–187.

[20]Narcisi, R., Trzcinski, E., Federico, C., Wlodyka, L., and Delorey, D., "The Gaseous and Plasma Environment Around the Space Shuttle," *Proceedings of the Shuttle Environment and Operations Meeting*, AIAA, Washington, DC, 1983, p. 183.

[21]Hunton, D. E., and Calo, J. M., "Low Energy Ions in the Shuttle Environment: Evidence for Strong Ambient-Contamination Interactions," *Planetary Space Sciences*, Vol. 33, Aug. 1985, p. 945.

[22]Bryson, R. J., Seiber, B. L., Bailey, A. B., and Wood, B. E., "Qualification Test of MSX Satellite Cryogenic Quartz Crystal Microbalances—Part 2," AEDC-TSR-91-V25, Nov. 1991.

[23]Wood, B. E., Seiber, B. L., Bertrand, W. T., and Uy, O. M., "Effects of Thin Cryo-Contaminant Films on Midcourse Space Experiment (MSX) Satellite Cryo-Optics," AIAA Paper 96-0221, Jan. 1996.

[24]Bryson, R. J., Bailey, A. B., Seiber, B. L., Bertrand, W. T., Jones, J. H., and Wood, B. E., "Cryogenic Quartz Crystal Microbalance: Characterization and Calibration for Midcourse Space Experiment," *Proceedings of the SPIE International Society of Optical Engineering, Optical System Contamination—Effects, Measurement and Control*, Vol. 1754, No. 22, 1992, p. 205.

[25]Bryson, R. J., Seiber, B. L., Bertrand, W. T., Jones, J. H., Wood, B. E., and Lesho, J. C., "Pre-Flight Testing of Thermoelectric Quartz Crystal Microbalances (TQCM) for Midcourse Space Experiment (MSX) Spacecraft," AEDC-TR-93-24, Feb. 1994.

[26]Bryson, R. J., Seiber, B. L., Bertrand, W. T., Jones, J. H., and Wood, B. E., "MSX Thermoelectric Quartz Crystal Microbalances—Calibration and Characterization," *Proceedings of the SPIE International Symposium on Optics, Imaging, and Instrumentation*, Vol. 2261, No. 17, 1994, p. 256.

[27]Lesho, J. C., Uy, O. M., Mehoke, D., and Wood, B. E., "Prediction of On-Orbit Temperatures for the MSX QCM Thermal Radiators," *Proceedings of the SPIE International Symposium on Optics, Imaging, and Instrumentation*, Vol. 2261, No. 20, 1994, p. 200.

[28]Allen, C. W., *Astrophysical Quantities*, 2nd ed., Athlone, London, 1976, pp. 190–244.

[29]Okabe, H., "Photodissociation of Nitric Acid and Water in the Vacuum Ultraviolet: Vibrational and Rotational Distributions of OH $^2\Sigma^+$," *Journal of Chemical Physics*, Vol. 72, No. 12, 1980, pp. 6642–6650.

[30]Lee, L. C., "OH ($^2S^+$-2P) Yield from H_2O Photodissociation in 1050–1370A," *Journal of Chemical Physics*, Vol. 72, April 1980, p. 4334.

[31]Stair, A. T., Jr., "MSX Design Parameters Driven by Targets and Backgrounds," *Johns Hopkins APL Technical Digest*, Vol. 17, No. 1, 1996, p. 11.

[32]Paxton, L. J., Meng, C.-I., Anderson, D. E., and Romick, G. J., "MSX—A Multiuse Space Experiment," *Johns Hopkins APL Technical Digest*, Vol. 17, No. 1, 1996, p. 19.

[33]Green, B. D., Rawlins, W. T., Mulhall, P. A., and Uy, O. M., "Optical Signatures of Particles in Space," *Optical Engineering* (to be published).

[34]Clifton, K. S., and Owens, J., "Optical Contamination Measurements on Early Shuttle Missions," *Applied Optics*, Vol. 27, Feb. 1988, p. 603.

[35]Green, B. D., and Ahmadjian, M. A., "Variable Shuttle Environment Around the Shuttle," *Applied Optics* (to be published).

[36]Barengoltz, J., "Particle Release Rates from Shuttle Orbiter Surfaces due to Micrometeorite Impact," *Journal of Spacecraft and Rockets*, Vol. 17, No. 1, 1980, p. 58.

F. S. Milos
Associate Editor